New insights on the kinetic analysis of isothermal data: the independence of the activation energy from the assumed kinetic model.

Pedro E. Sánchez-Jiménez[*], *Antonio Perejón, Luis A. Pérez-Maqueda, José M. Criado.*

Instituto de Ciencia de Materiales de Sevilla, C.S.I.C.-Universidad de Sevilla, C. Américo Vespucio nº49, 41092 Sevilla, Spain

Abstract

Isothermal experiments are widely employed to study the kinetics of solid state reactions or processes in order to extract essential kinetic information needed for modeling the processes at an industrial scale. The kinetic analysis of isothermal data requires finding or assuming a kinetic function that can properly fit the evolution of reaction rate with time so that the resulting parameters, i.e. the activation energy and the preexponential factor, can be considered reliable. In the present work, we demonstrate using both simulated and experimental data that the kinetic analysis of a set of isothermal plots obtained at different temperatures, considering a single step solid state reaction, necessarily leads to the real activation energy, regardless the mathematical function selected for performing the kinetic analysis. This makes irrelevant the election of the kinetic function used to fit the experimental data and greatly facilitates the estimation of the activation energy for any single process.

Keywords: Kinetic Analysis, Isothermal; Kinetic Model; Activation Energy; Process Modeling

[*]Corresponding author. Tel +34954489548 Fax +34954460665
e-mail address: pedro.enrique@icmse.csic.es

1. Introduction

Kinetic analysis is widely employed as a tool for obtaining the essential knowledge needed for modeling processes on an industrial scale. This is also true in the field of energy conversion and production, with an important number of papers published every year in which the main objective is determining the kinetics governing processes such as pyrolysis, gasification, combustion or thermal decomposition in order to optimize operating conditions [1-14]. The experimental data are usually collected under isothermal or linear heating conditions. While linear heating rate experiments provide quickness and simplicity, in many studies such as those involving long-term aging at operation temperatures [15-17], oxidation processes [18-20], reaction progress followed by spectral or DRX peak intensity measurements [21-23], chemical looping processes [1, 3, 11, 24] or those set-ups that try to replicate industrial operation conditions [9, 12, 13], isothermal experiments are still the most convenient or even feasible option. Moreover, isothermal experiments present the distinct advantage of a higher capability for kinetic mechanism discrimination due to the fact that the shape of the integral α-time curve is directly related to the obeyed model [25, 26]. Thus, the α-time traces of phase boundary controlled reaction (so called "n order" reactions) are convex, the diffusion controlled reactions are concave and those whose rate is controlled by the formation and growth of nuclei (Avrami-Erofeev models) have sigmoidal shape. On the other hand, the α-temperature plots recorded under rising temperature are always sigmoidal-shaped, whatever the reaction kinetic model [27, 28]

A former review [29] on the kinetic dehydroxylation of kaolinite found that similar activation energies had been reported by different authors despite the proposal of different kinetic models. An analysis of those experimental data assuming a set of different kinetic models revealed that the activation energies obtained were independent of the kinetic model previously assumed, although no explanation was given. If such behavior was generalized, it would constitute an extraordinary advantage since it is generally assumed that the activation energy obtained by a

kinetic analysis is dependent on the kinetic law used to fit the experimental data [27, 30, 31] . Thus, authors must spend a great deal of effort to determine the kinetic function most adequate to the process under study in order to assure a reliable set of kinetic parameters [27]. In the present work we explore the influence the kinetic law selected to fit the experimental data has on the activation energy yielded by the kinetic analysis of a set of isothermal curves recorded at different temperatures. It is demonstrated first theoretically and then analyzing sets of both simulated and experimental data, that the activation energy obtained by this kind of analysis would always be the correct one, regardless the mathematical function selected for fitting the data.

2. Experimental

Thermal degradation experiments were carried out using polytetrafluoroethylene (Aldrich, product number 182478) at temperatures of 480, 490 and 500 ºC in a Q5000IR TA Instruments TGA (TA Instruments, Crawley, UK) connected to a gas flow system to work in inert atmosphere equipment under 100 mL min^{-1}. Samples sizes of ~20 mg were placed in a platinum crucible and heated at 300 ºC min^{-1} to the final temperature in order to avoid mass loss before the steady state is attained.

3. Theory

It is well known that the kinetics of a solid state reaction, in conditions far from the equilibrium, can be described by the general equation:

$$\frac{d\alpha}{dt} = kf(\alpha) \qquad (1),$$

where *t* represents the time, α is the extent of reaction and *k* is the rate constant, which depends on the temperature according to the Arrhenius equation, $k=Aexp(-E_a/RT)$. The kinetic model, *f(α),* is a function describing the relationship between the reaction rate and the reacted fraction. An ample selection of *f(α)* functions have been published along the last decades, ranging from the widely employed first or n^{th} order laws to more sophisticated diffusion or nucleation models [32-34]. It is important to remark that Eq. (1) does not consider any particular heating schedule so it should be fulfilled whatever the time-temperature program employed for obtaining the experimental data. Additionally, the reacted fraction or conversion α can be established using data extracted with any technique measuring a property that can be directly related to the reaction rate, most usually the mass loss recorded by thermogravimetry. The standard isothermal method of kinetic analysis follows a model-fitting approach[27]. Thus, a series of isotherms are recorded at different temperatures and the extracted experimental data are fitted to a set of different kinetic models, according to the following equations, which are obtained by integrating Eq (1):

$$\int_0^\alpha \frac{d\alpha}{f(\alpha)} = \int_0^t k dt \quad (2a)$$

$$g(\alpha) = kt \quad (2b),$$

where *g(α)* is the integral form of the kinetic model. The plot of *g(α)*versus the reaction time (provided that the time for reaching the temperature steady state is negligible with regards to the elapsed time) leads to a straight line whose slope is the rate constant, *k*. Then, given the Arrhenius dependence of the rate constant with the temperature, the activation energy can be subsequently calculated by plotting the logarithm of the rate constants versus the reverse of their corresponding temperatures:

$$\ln k = \ln A - E_a/RT \quad (3)$$

Let us assume the experimental kinetic data are fitted with a G(α) function different from the one really obeyed by the reaction, g(α), regardless of the quality of the resulting regression coefficient. In such case, an apparent rate constant, k_a, would be obtained from the plot of G(α) as a function of *t* according to the following equation:

$$G(\alpha) = k_a t \quad (4),$$

The comparison of Eqs (2b) and (4) leads to the conclusion that the acceptance of a reasonable linear correlation between G(α) and t necessarily implies to accept a linear correlation between G(α) and g(α), that would be expressed according to the following equation:

$$G(\alpha) = a g(\alpha) + b \quad (5),$$

a and *b* being constants.

It can be concluded from Eqs. (2b), (4) and (5) that, whatever would be the temperature, the apparent constant reaction rate, k_a is related with the actual one, *k*, through the following relationships:

$$\frac{dG(\alpha)}{dt} = k_a = a\frac{dg(\alpha)}{dt} = ak \quad (6).$$

Eq. (6) shows that $k_a = ak$. Moreover, taking into account that *k* fits the Arrhenius equation, it follows:

$$k_a = ak = aAe^{-E/RT} \quad (7),$$

that could be rearranged in the following form:

$$\frac{-dlnk_a}{d(1/T)} = \frac{-dlnk}{d(1/T)} = E/R \quad (8)$$

Thus, Eq. (8) clearly demonstrates that the activation energy determined from a set of isothermal α-time plots obtained at different temperatures is independent of the kinetic model previously assumed for performing the kinetic analysis.

4. Kinetic analysis of simulated isothermal curves

The time at which a given α value is reached at a certain temperature T can be determined, according to Eq. (2b), from the following expression:

$$t = \frac{g(\alpha)}{Ae^{-E/RT}} \quad (9)$$

Thus, Eq. (9) was used to numerically construct two sets of simulated curves assuming temperatures of 250, 265, 275 and 300 ºC. Figure 1a includes a set of isotherms simulated according to the following kinetic parameters: E=200 kJ/mol, $A=10^{16}$ min^{-1} and a first order kinetic model (F1). On the other hand, isotherms in Figure 1b were constructed assuming the same activation energy and pre-exponential factor as the previous set and an Avrami nucleation kinetic model (A2). The figure clearly shows how the first order trace is convex while the nucleation-driven trace is sigmoidal, as aforementioned. Then, the data from all the curves in Figure 1 were linearly fitted to several theoretical kinetic models, as per Eq (2b), producing the rate constant values listed in Tables 1 and 2, together with their corresponding correlation coefficients. In order to better replicate the analysis procedures most commonly employed in the literature, the fit was limited to data comprising the conversion range $0.1 \leq \alpha \leq 0.9$ since the extreme ranges are more sensitive to experimental errors. Figure 2 includes a selection of plots constructed using data from the 265 ºC isothermal curve, providing a clear picture of the results obtained. The linear fits from which slope the rate constants are determined are also marked in the Figure. As expected, only the correct *g(α)* function produces a flawless linear fit whereas

the fit to incorrect models yield non-linear plots with different slopes and, therefore, lead to different rate constants. Nevertheless, it is worth mentioning that 5 out of the 8 models tested yielded significant correlation coefficients, over 0.99. Even more striking are the conclusions reached when the activation energy is determined for each set of rate constants (Tables 1 and 2) as per Eq. (3). Table 3 lists the activation energies and pre-exponential factors obtained, depending on the model used to construct the simulated curves and the model used to fit the data. Results are identical for every case, with the analysis yielding the correct activation energy regardless the model assumed. Thus, the erroneous selection of a kinetic law, and consequently, the erroneous estimation of the rate constants have no influence whatsoever on the obtained activation energy. On the other hand, the pre-exponential factors present a slight variability as it is expected from Eq. (7), although it is still well within the accepted error range given the high numerical value of such constant. It should be warned that any prediction attempt requires the knowledge of correct kinetic model driving the proccess. Thus, for a given temperature, each kinetic triplet in Table 3 will produce a different α-time curve, with only the right model been able to accurately predict the experimental curve. Nevertheless, it is still possible to make reliable predictions from the model-independent E values obtained by the isothermal method by employing Vyazovkin's isoconversional equation.[35]

5. Kinetic analysis of experimental isothermal curves

Next, for further confirmation, real experimental data are tested. Figure 3 includes three isothermal curves, corresponding to the decomposition of polytetrafluoroethylene (Aldrich, product number 182478) recorded at temperatures of 480, 490 and 500 ºC in a Q5000IR TA Instruments TGA equipment under a 100 mL min^{-1} flow of N_2. The plots of $g(\alpha)$ versus the reaction time, as per Eq (2b), for each isothermal curve were built using eight different kinetic models. A selection of these plots is shown as examples in Figure 4. The rate constants, as

158 directly calculated from the slope of the plots, are included in Table 4, as well as the activation
159 energies determined using each set of rate constants, as previously described. Additionally, the
160 plots of the rate constants versus the reverse of the temperature (as per Eq. (3)), from which the
161 activation energies are calculated, are included in Figure 5. These results indicate that, as
162 predicted by the mathematical development presented in a previous section, the same value for
163 the activation energy, 261±1 kJ/mol, is reached whatever the kinetic model used to fit the data.
164 The activation energy here obtained is in agreement with that estimated in a previous study
165 using the same material and employing a combined approach based on bothmodel-fitting and
166 isoconversional methods, thus confirming the validity of the results.[36] Additionally, as it
167 happened with the simulated curves, four out of eight models can fit the experimental data with
168 reasonable correlation coefficients.

169 This finding entails significant implications. The fact that the correct activation energy of a
170 single process would always be obtained from a set of isotherms regardless of the kinetic model
171 chosen to fit the data permits the isothermal method of kinetic analysis to provide the activation
172 energy of any single step reaction without needing any previous knowledge regarding the
173 reaction mechanism. In any case, heat and mass transfer limitations typical of isothermal
174 experiments must still be considered in the experiments design since they will inevitably
175 produce interferences with the real proccess if not adequately minimized. The ability of the
176 method to yield the correct activation energy regardless of the model used is especially
177 interesting if we consider that most reactions will rarely follow faithfully any theoretical
178 models, which were built upon several ideal assumptions and constraints which are seldom
179 fulfilled in real reactions. For instance, inhomogenous distribution in size and particle shape
180 have been shown to have an important effect on the shape of the experimental curves.[37] Such
181 deviations would have consequences in model-fitting methods of kinetic analysis of linear
182 heating rate experiments because the activation energy and the pre-exponential factors provided

are heavily dependent on the kinetic model used for the fitting. [31, 38, 39] On the other hand, as shown here, the activation energy and pre-exponential factors provided by the isothermal method are independent of the model used to fit the experimental data, hence preventing the distorting effect of non-ideal models or inhomogenous materials.

6. Conclusions

It has been proven that the actual activation energy of any single step solid state reaction can be determined from a set of isothermal experiments regardless of the kinetic model of function obeyed by the reaction and/or the kinetic equation previously assumed for performing the kinetic analysis. Thus, the isothermal method of kinetic analysis behaves at all effects as a model-free since the activation energy and the pre-exponential factor can be calculated without a previous knowledge of the kinetic model. Moreover, the kinetic parameters thus obtained would be representative of the reaction even when none of the theoretical models could closely represent the studied process.

ACKNOWLEDGEMENTS

Financial support from projects TEP-7858 and TEP-1900 from Junta de Andalucía, CTQ2011-27626 from the Spanish Ministerio de Economía y Competitividad and FEDER funds is acknowledged. Additionally, one of the authors (PESJ) is supported by a Juan de la Cierva grant.

References

1. Grasa, G.; Martinez, I.; Diego, M. E., et al., *Energ Fuel.* **2014,** *28* (6), 4033-4042.
2. Wang, C.; Dou, B. L.; Song, Y. C., et al., *Energ Fuel.* **2014,** *28* (6), 3793-3801.

206 3. Martinez, I.; Grasa, G.; Murillo, R., et al., *Energ Fuel.* **2012,** *26* (2), 1432-1440.
207 4. Varhegyi, G.; Bobaly, B.; Jakab, E., et al., *Energ Fuel.* **2011,** *25*, 24-32.
208 5. Saddawi, A.; Jones, J. M.; Williams, A., et al., *Energ Fuel.* **2010,** *24*, 1274-1282.
209 6. Koga, N.; Yamada, S.; Kimura, T., *J. Phys. Chem. C.* **2013,** *117* (1), 326-336.
210 7. Perejon, A.; Sanchez-Jimenez, P. E.; Gil-Gonzalez, E., et al., *Polym. Degrad. Stabil.* **2013,** *98* (9),
211 1571-1577.
212 8. Noda, Y.; Koga, N., *J. Phys. Chem. C.* **2014,** *118* (10), 5424-5436.
213 9. Yuan, S. A.; Chen, X. L.; Li, J., et al., *Energ Fuel.* **2011,** *25* (5), 2314-2321.
214 10. Roberts, D. G.; Hodge, E. M.; Harris, D. J., et al., *Energ Fuel.* **2010,** *24*, 5300-5308.
215 11. Abanades, S.; Chambon, M., *Energ Fuel.* **2010,** *24*, 6667-6674.
216 12. Jing, X. D.; Yan, G. X.; Zhao, Y. H., et al., *Energ Fuel.* **2014,** *28* (8), 5396-5405.
217 13. Yue, L.; Qin, X. M.; Wu, X., et al., *Energ Fuel.* **2014,** *28* (7), 4523-4531.
218 14. Wu, W. X.; Mei, Y. F.; Zhang, L., et al., *Energ Fuel.* **2014,** *28* (6), 3916-3923.
219 15. Richaud, E.; Le Gac, P. Y.; Verdu, J., *Polym. Degrad. Stabil.* **2014,** *102*, 95-104.
220 16. Grioui, N.; Halouani, K.; Agblevor, F. A., *Energ. Sustainable Development.* **2014,** *21*, 100-112.
221 17. Celina, M.; Gillen, K. T.; Assink, R. A., *Polym. Degrad. Stabil.* **2005,** *90* (3), 395-404.
222 18. Chen, X.; Hou, P. Y.; Jacobson, C. P., et al., *Solid State Ionics.* **2005,** *176* (5-6), 425-433.
223 19. Cai, M.; Ruthkosky, M. S.; Merzougui, B., et al., *J. Power Sources.* **2006,** *160* (2), 977-986.
224 20. Raj, R.; An, L. N.; Shah, S., et al., *J. Am. Ceram. Soc.* **2001,** *84* (8), 1803-1810.
225 21. Huang, Y. F.; Chiueh, P. T.; Kuan, W. H., et al., *Appl. Energ.* **2013,** *110*, 1-8.
226 22. Choi, S. Y.; Mamak, M.; Speakman, S., et al., *Small.* **2005,** *1* (2), 226-232.
227 23. Sung, Y. M.; Lee, Y. J.; Park, K. S., *J. Am. Ceram. Soc.* **2006,** *128* (28), 9002-9003.
228 24. Monazam, E. R.; Breault, R. W.; Siriwardane, R., *Energ Fuel.* **2014,** *28* (8), 5406-5414.
229 25. Sanchez-Jimenez, P. E.; Perez Maqueda, L. A.; Perejón, A., et al., *J. Phys. Chem. C.* **2012,** *116*
230 (21), 11797–11807.

26. Sanchez-Jimenez, P. E.; Perez-Maqueda, L. A.; Perejon, A., et al., *Cellulose.* **2011,** *18* (6), 1487-1498.

27. Vyazovkin, S.; Burnham, A. K.; Criado, J. M., et al., *Thermochim. Acta.* **2011,** *520* (1-2), 1-19.

28. Sánchez-Jiménez, P. E.; Pérez-Maqueda, L. A.; Perejón, A., et al., *Polym. Degrad. Stabil.* **2011,** *96* (5).

29. Criado, J. M.; Ortega, A.; Real, C., et al., *Clay Minerals.* **1984,** *19* (4), 653-661.

30. Criado, J. M.; Ortega, A., *J. Therm. Anal.* **1984,** *29* (6), 1225-1236.

31. Sanchez-Jimenez, P. E.; Perez-Maqueda, L. A.; Perejon, A., et al., *Resour. Conserv. Recy.* **2013,** *74*, 75-81.

32. Brown, M. E., *Introduction to Thermal Analysis*. 2nd ed.; Kluwer: Dodrecht, 2001.

33. Sanchez-Jimenez, P. E.; Perez-Maqueda, L. A.; Perejon, A., et al., *Polym. Degrad. Stabil.* **2010,** *95* (5), 733-739.

34. Ortega, A.; Perez-Maqueda, L. A.; Criado, J. M., *Thermochim. Acta.* **1996,** *283*, 29-34.

35. Vyazovkin, S.; Dranca, I.; Fan, X.; Advincula R., *Macromol. Rapid. Commun.* **2004,** *25*, 498.

36. Sanchez-Jimenez, P. E.; Perez-Maqueda, L. A.; Perejon, A., et al., *Polym. Degrad. Stabil.* **2009,** *94* (11), 2079-2085.

37. Koga, N.; Criado, J. M., *J. Am. Ceram. Soc.* **1998,** *81* (11), 2901-2909.

38. Sanchez-Jimenez, P. E.; Perez-Maqueda, L. A.; Perejon, A., et al., *Chem. Central Journal.* **2013,** *7*.

39. Sanchez-Jimenez, P. E.; Rodriguez-Laguna, M. D.; Perez-Maqueda, L. A., et al., *Appl. Energ.* **2014,** *125*, 132-135.

Con formato: Español (alfab. internacional)

Con formato: Español (alfab. internacional)

Figure Captions

Figure 1. Isothermal curves simulated according to the following kinetic parameters: E=200kJ/mol, $A=10^{16}$ min^{-1} and (a) F1 kinetic model, $f(\alpha)=(1-\alpha)$ or (b) A2 Avrami model, $f(\alpha)=2(1-\alpha)(-\ln(1-\alpha))^{0.5}$.

Figure 2. Fit of the 265ºC isothermal curves simulated assuming (a) F1 and (b) A2 models to a set of different kinetic models.

Figure 3. Isothermal curves corresponding to the degradation of PTFE, recorded at 480, 490 and 500ºC.

Figure 4. Fit of the PTFE degradation isothermal curves in Figure 3 to four different kinetic models: first order (F1), phase boundary controlled (R2), two-dimnsional diffusion (D2) and nucleation (A2).

Figure 5. Plot of ln*k* versus the reverse of their corresponding temperature, constructed for every set of rate constants in Table 4. Activation energy is extracted from the slope of the plots, being identical in every case.

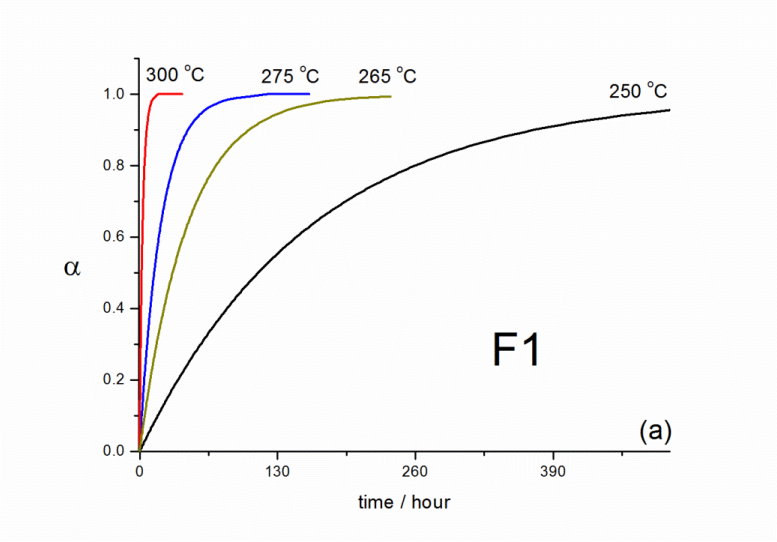

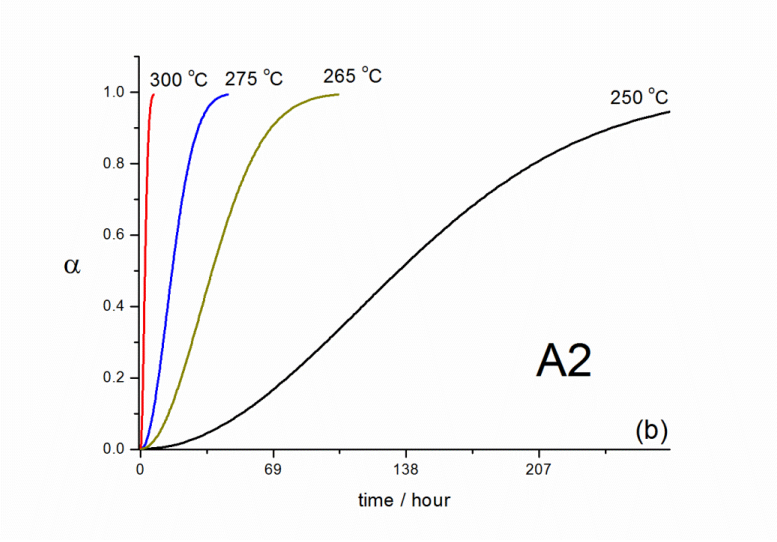

Figure 1. Isothermal curves simulated according to the following kinetic parameters: E=200kJ/mol, A=10^{16} min^{-1} and (a) F1 kinetic model, f(α)=(1-α) and (b) A2 Avrami model, f(α)=2(1-α)(-ln(1-α))$^{0.5}$.

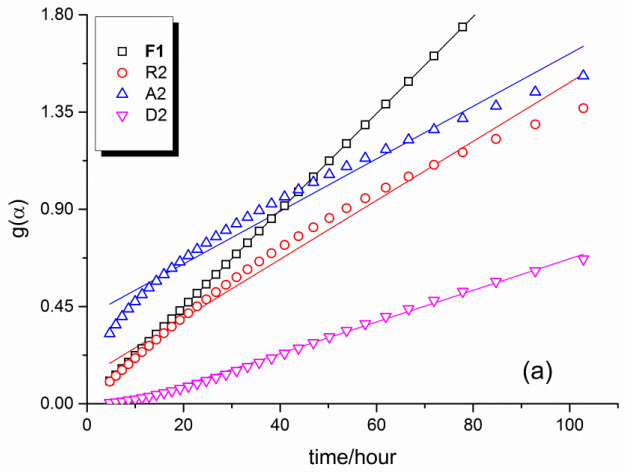

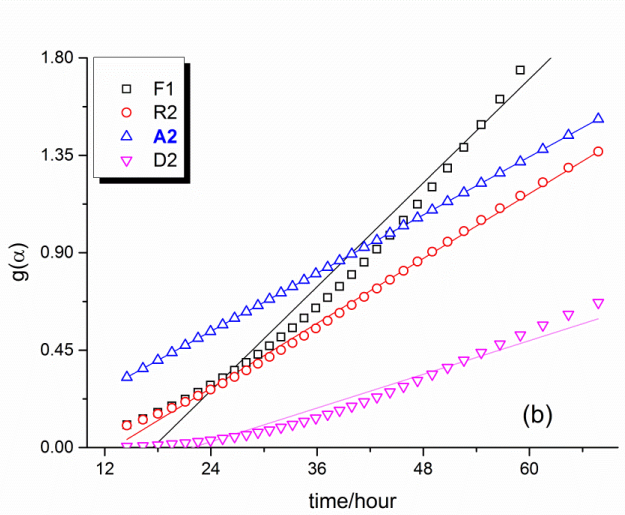

Figure 2. Fit of the 265ºC isothermal curves simulated assuming (a) F1 and (b) A2 models to a set of different kinetic models.

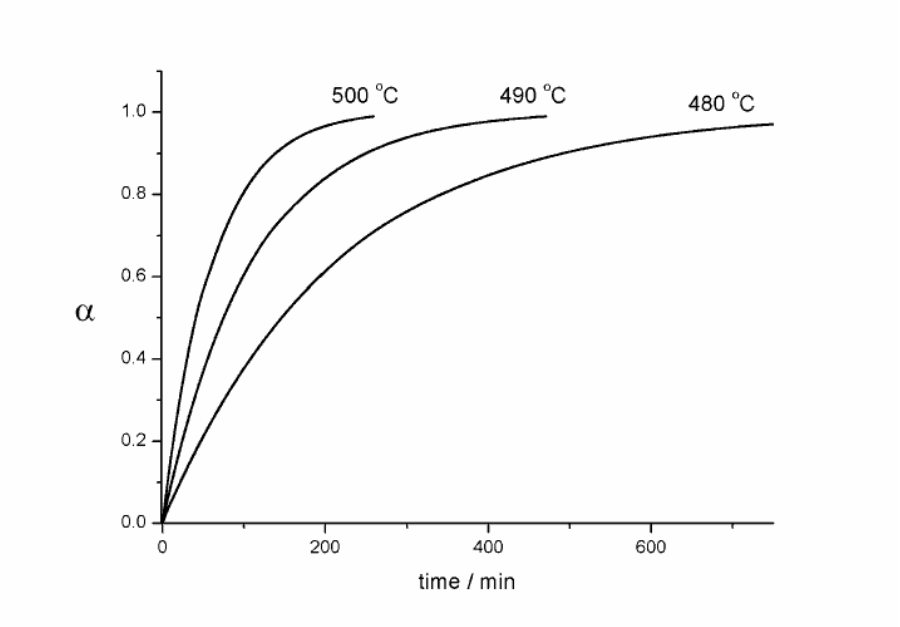

Figure 3. Isothermal curves corresponding to the degradation of PTFE, recorded at 480, 490 and 500ºC.

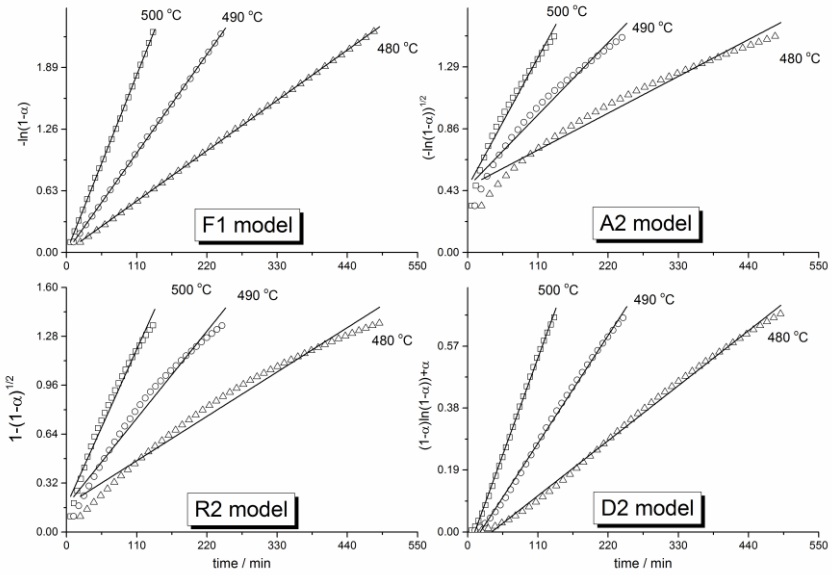

Figure 4. Fit of the PTFE degradation isothermal curves in Figure 3 to four different kinetic models: first order (F1), pase boundary controlled (R2), two-dimensional diffusion (D2) and nucleation (A2).

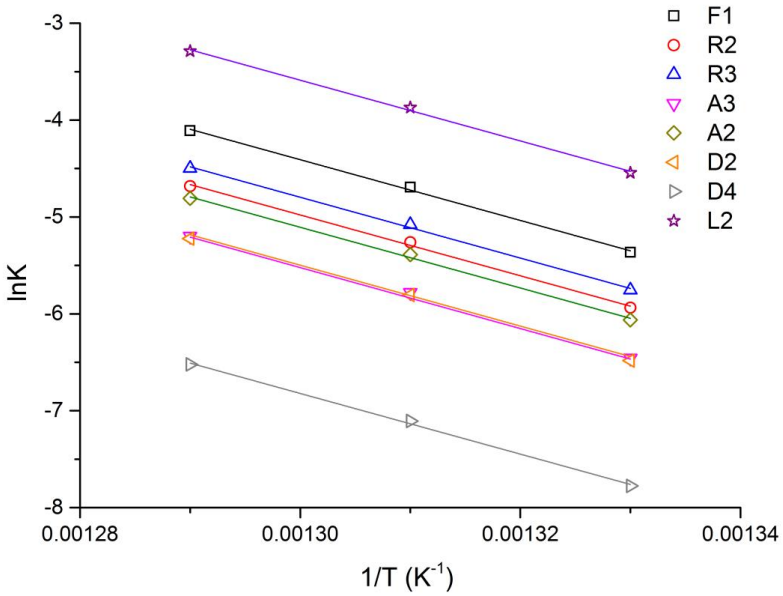

Figure 5. Plot of ln*k* versus the reverse of their corresponding temperature, constructed for every set of rate constants in Table 4. Activation energy is extracted from the slope of the plots, being identical in every case.

Table 1. Rate constants and correlation factors obtained from fitting simulated curves in Figure 1a (assuming a F1 model) to different kinetic models, according to Eq. (2a).

Model Fitted to	250°C		265°C		275°C		300°C	
	k (min^{-1})	r^2	k (min^{-1})	r^2	k (min^{-1})	r^2	k (min^{-1})	r^2
F1	0.0062	1.000	0.0224	1.000	0.0507	1.000	0.3441	1.000
R2	0.0038	0.981	0.0136	0.980	0.0309	0.980	0.2097	0.980
R3	0.0044	0.991	0.0160	0.991	0.0362	0.991	0.2456	0.991
A2	0.0034	0.970	0.0122	0.970	0.0275	0.970	0.1868	0.970
A3	0.0024	0.944	0.0085	0.944	0.0192	0.944	0.1305	0.944
D2	0.0020	0.996	0.0073	0.996	0.0165	0.996	0.1124	0.996
D4	0.0005	0.993	0.0020	0.993	0.0044	0.993	0.0300	0.993
L2	0.0145	0.996	0.0524	0.996	0.1186	0.996	0.8060	0.996

Table 2. Rate constants and correlation factors obtained from fitting the simulated curves in Figure 1b (assuming a A2 model) to different kinetic models, according to Eq. (2a).

Model Fitted to	250°C		265°C		275°C		300°C	
	k (min^{-1})	r^2	k (min^{-1})	r^2	k (min^{-1})	r^2	k (min^{-1})	r^2
F1	0.0111	0.970	0.0400	0.970	0.0905	0.970	0.6147	0.970
R2	0.0069	0.997	0.0250	0.997	0.0565	0.997	0.3836	0.997
R3	0.0080	0.992	0.0290	0.992	0.0656	0.992	0.4458	0.992
A2	0.0062	1.000	0.0224	1.000	0.0507	1.000	0.3441	1.000
A3	0.0044	0.996	0.0158	0.996	0.0358	0.996	0.2430	0.996
D2	0.0036	0.953	0.0130	0.953	0.0293	0.953	0.1994	0.953
D4	0.0010	0.936	0.0034	0.936	0.0078	0.936	0.0529	0.936
L2	0.0263	0.988	0.0947	0.988	0.2143	0.988	1.4563	0.988

Table 3. Activation energies, pre-exponential factors and correlation coefficients obtained from the plot of the different rate constants in Tables 1 and 2 versus the reverse of their corresponding temperature, as per Eq.(3).

	Model used to simulate the curves					
	F1			**A2**		
Model fitted to	**E (kJ mol^{-1})**	**A (min^{-1})**	**r^2**	**E (kJ mol^{-1})**	**A (min^{-1})**	**r^2**
F1	200	$5x10^{16}$	1.000	200	$1x10^{17}$	1.000
R2	200	$5x10^{16}$	1.000	200	$6x10^{16}$	1.000
R3	200	$4x10^{16}$	1.000	200	$8x10^{16}$	1.000
A2	200	$3x10^{16}$	1.000	200	$6x10^{16}$	1.000
A3	200	$2x10^{16}$	1.000	200	$4x10^{16}$	1.000
D2	200	$2x10^{16}$	1.000	200	$4x10^{16}$	1.000
D4	200	$5x10^{15}$	1.000	200	$1x10^{16}$	1.000
L2	200	$1x10^{17}$	1.000	200	$3x10^{17}$	1.000

Table 4. Rate constants and correlation factors calculated from the fit of the experimental curves corresponding to the degradation of PTFE (Figure 3) to a set of theoretical kinetic models. The activation energy and correlation coefficients obtained from the plot of the rate constants versus the reverse of the temperature (Eq.(3)) are also included.

	480ºC		**490ºC**		**500ºC**		**Result of Isothermal analysis**	
Model Fitted to	**k (min^{-1})**	**r^2**	**k (min^{-1})**	**r^2**	**k (min^{-1})**	**r^2**	**E (kJ mol^{-1})**	**r^2**
F1	0.0047	1.000	0.0092	1.000	0.0164	0.999	261±10	0.997
R2	0.0026	0.978	0.0052	0.979	0.0093	0.982	261±11	0.996
R3	0.0032	0.990	0.0062	0.990	0.0111	0.993	261±11	0.996
A2	0.0023	0.973	0.0046	0.974	0.0082	0.977	260±11	0.996
A3	0.0016	0.951	0.0031	0.952	0.0055	0.955	261±12	0.996
D2	0.0015	0.997	0.0030	0.998	0.0054	0.998	262±11	0.996
D4	0.0004	0.997	0.0008	0.997	0.0015	0.997	260±10	0.997
L2	0.0106	0.996	0.0208	0.997	0.0373	0.997	261±10	0.996

342

343

344